Flexure Systems based on a Symmetric Diaphragm Flexure

Shorya Awtar, Alexander H. Slocum
Precision Engineering Research Group, Massachusetts Institute of Technology
77 Massachusetts Avenue, 3-445, Cambridge MA 02139
shorya@mit.edu, slocum@mit.edu

Abstract

This paper presents a symmetric diaphragm flexure as an improvement over the conventional design, which suffers from parasitic error motions. Tradeoffs in the performance of diaphragm flexure geometries are discussed qualitatively and quantitatively. Variations of the proposed geometry are suggested to increase range of motion and tailor the mechanism's Center of Stiffness. The symmetric diaphragm flexure is used as a building block to construct other flexure systems such as flexible couplings and linear bearings. A linear force-displacement model for a curved beam is presented that allows analytical prediction and evaluation of the proposed flexure systems.

Keywords: Diaphragm Flexure, Flexible Coupling, Linear Bearing, Curved-beam Analysis

Introduction

Diaphragm flexures are commonly used to provide precise out-of-plane motions in various applications such as voice-coil actuators, pressure sensors, flow control, flexible couplings, MEMS devices, and frictionless linear bearings. A typical planer diaphragm flexure, comprising of an inner diaphragm, an outer frame, and intermediate flexure support units, offers three out-of-plane Degrees of Freedom (DOF) and three in-plane Degrees of Constraint (DOC). As in any flexure design, there exist performance tradeoffs between the quality of DOF and DOC [1]. While the traditional design [2-4], shown in Fig.1a, provides the desirable attributes of high in-plane stiffness and useful out-of-plane motion range, it is prone to a rotation about the Z-axis associated with Z translation. This parasitic error motion [1] is a consequence of the fact that the flexure units in this rotationally asymmetric design are fixed-free beams. To maintain the beam arc length during a Z translation, the free end of each beam moves towards its respective fixed end, resulting in an undesirable rotation of the diaphragm.

Although the alternate design of Fig.1b is free of this rotation because of its symmetric geometry, it is highly over-constrained in the out-of-plane directions. The flexure units in this case are similar to fixed-fixed beams, which suffer from a nonlinear stress-stiffening effect [1]. Thus, an attempt to improve the quality of a DOC significantly compromises the motion range along DOF. In general, for diaphragm flexures, the requirements of low parasitic motions along DOC, large range of motion along DOF, and high stiffness along DOC are mutually conflicting. In this paper, we present a symmetric diaphragm geometry, which offers an optimal overall performance, and may be used as a building block in the construction of other flexure systems such as torsion couplings, multi-DOF stages, and linear bearings.

Symmetric Diaphragm Flexure and Variations

Fig.1c illustrates the proposed symmetric diaphragm flexure comprising of multiple folded-beam pairs [5-6]. While the rotational symmetry eliminates the parasitic rotation of the diaphragm, the folded-beam geometry relieves any axial stress associated with out-of-plane motions. Furthermore, the increased effective length of the folded-beams also provides a large range motion along the DOF. However, this geometry also reduces the rotational stiffness along the Z-axis. Nonlinear elastokinematic effects in a folded-beam unit are more dominant as compared to a simple beam, and cause its stiffness along the beam length to drop at a relatively higher quadratic rate with increasing out-of-plane motions. From the diaphragm flexure's DOC standpoint, this effect influences the stiffness along the tangential directions but not the radial directions. Therefore, it is important to have at least three pairs of folded-beams, which will ensure high stiffness along any planer translation. However, for a pure Z rotation, all the folded-beam pairs are loaded along the beam length, and the high radial stiffness does not come into play. While, fundamentally, only three flexure units, either simple beams or folded-beams pairs, are needed to adequately support the central diaphragm, four or more units may be used as well. The phenomenon of elastic averaging not only ensures that there is no over-constraint, but also reduces the variation of planer translation stiffness with direction and makes the design more robust against geometric flaws.

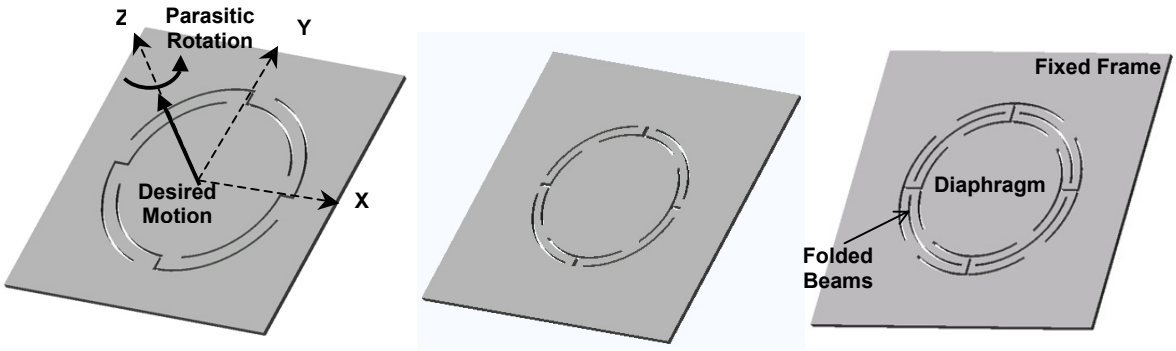

Fig.1 Diaphragm Flexures a) Traditional Design b) Over-constrained Symmetric c) Optimal Symmetric

Nevertheless, increasing the number flexure support units also reduces the individual beam length, making the design relatively stiffer along the DOF. In order to increase compliance, and therefore range of motion, along these directions, the effective beam length of each flexure unit can be further increased by incorporating multiple beam folds, as shown in Fig.2a. However, the rotational stiffness about the Z-axis deteriorates with each additional beam fold. Obviously, the symmetric diaphragm flexure design needs to be tailored to meet the specific requirements of a given application, since the relevant performance measures cannot all be maximized simultaneously.

Because of its symmetry, the center of stiffness (COS) of the proposed diaphragm flexure, with respect to out-of-plane loads, lies at the center of the diaphragm. But if necessary, the COS of the mechanism can be shifted to any arbitrary point in the plane of the flexure by varying the blade width and/or thickness of the folded-beams, as illustrated in Fig.2b. Nevertheless, symmetry of each folded-beam pair is preserved about its respective midpoint, and hence parasitic Z rotation is still avoided.

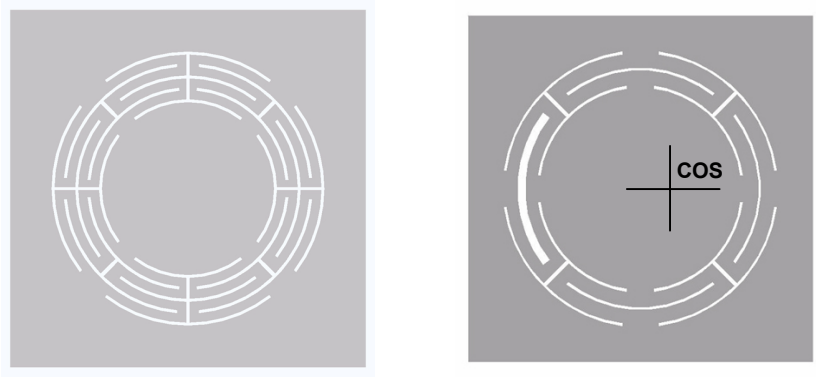

Fig.2 Diaphragm Flexure Variations a) Increased Compliance b) Shifted Center of Stiffness

Flexure Stages based on Diaphragm Flexure

Since all the diaphragm flexures presented in the previous section provide three DOC and three DOF, they can be used as monolithic versions of universal joints with an additional DOF along Z translation. Furthermore, two or more diaphragm flexure modules may be connected in series along a common Z-axis to yield a single torsional DOC flexure system. The fact that this flexure system provides a pure rotational constraint makes it suitable for use as a 5DOF torque coupling [5-6]. One possible design embodiment of this idea is shown in Fig. 3a. Two shafts can be attached to either end of this tuna-can shaped coupling constructed from a single formed piece of sheet metal. The performance of this coupling in terms of torsional stiffness and amount of misalignment allowed between the two shafts is obviously dependent on the force-displacement characteristics of the diaphragm flexure module.

Another useful flexure system, presented in Fig.3b, comprises of two parallel diaphragm flexure modules, spaced along the Z-axis; a housing rigidly attached to the outer frames of the two modules; and a reciprocator attached to the inner diaphragms of both modules. This arrangement results in a high-precision linear bearing [5-6], with a low compliance, zero friction and a relatively large stroke along the Z direction, and high stiffness along all other directions. Minimal Z rotation and high thermal stability are

desirable in a linear bearing, making the proposed symmetric diaphragm flexure an ideal building block. The range of motion is limited by the minimum acceptable rotational stiffness about the Z-axis. Multiple parallel diaphragms may be used in this linear bearing arrangement to improve DOC stiffness without causing over-constraints.

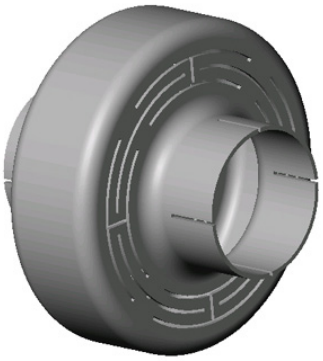

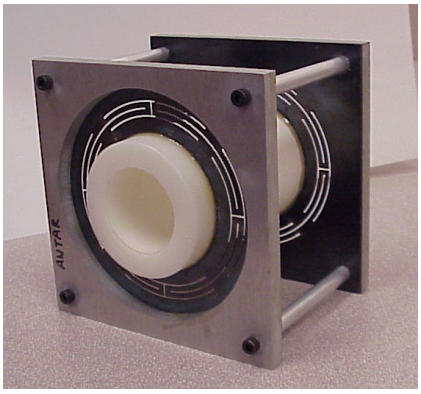

Fig.3 a) Five-DOF Flexible Coupling b) Single-DOF Linear Bearing

Analysis

A simple curved-beam, illustrated in Fig.4, forms the basic flexure unit in all the flexure systems discussed in this paper. Therefore, we proceed to derive the force-displacement characteristics of this curved-beam assuming standard Euler-Bernoulli approximations. A cylindrical coordinate system (r-β-z), as shown below, suits the curved-beam and subsequent diaphragm flexure geometries.

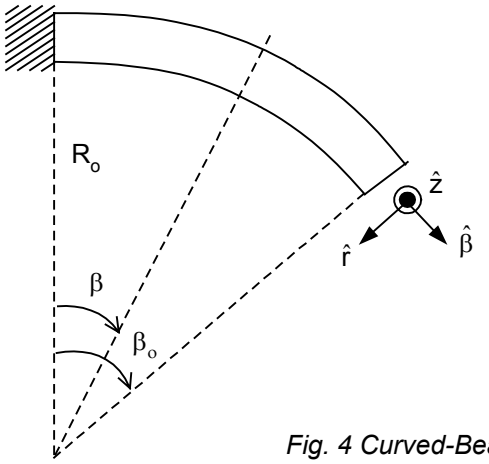

$$M(\beta_o) = M_r^o\ \hat{r} + M_\beta^o\ \hat{\beta} + M_z^o\ \hat{z}$$
$$F(\beta_o) = F_z^o\ \hat{r} + F_\beta^o\ \hat{\beta} + F_z^o\ \hat{z}$$
$$u(\beta_o) = u_r^o\ \hat{r} + u_\beta^o\ \hat{\beta} + u_z^o\ \hat{z}$$
$$\theta(\beta_o) = \theta_r^o\ \hat{r} + \theta_\beta^o\ \hat{\beta} + \theta_z^o\ \hat{z}$$

Fig. 4 Curved-Beam Model

Neglecting the non-linearities associated with geometric compatibility, the governing relationships for the curved beam, with respect to the system variable β are given by

$$\theta_r'(\beta) = -\theta_\beta(\beta) + \frac{R_o M_r(\beta)}{EI_b} \quad ; \quad \theta_\beta'(\beta) = \theta_r(\beta) + \frac{R_o M_\beta(\beta)}{GI_t} \quad ; \quad u_z(\beta) = R_o\theta_r(\beta)$$

$$\Rightarrow u_z'''(\beta) + u_z'(\beta) = R_o^2\left[\frac{M_r'(\beta)}{EI_b} - \frac{M_\beta(\beta)}{GI_t}\right]$$

The curved beam geometry results in an interesting coupling between bending and torsion, as evident in the above expressions. Either bending or twisting moment at the beam tip results in differing degrees of bending as well as torsion along beam length. Assuming force-equilibrium in the undeformed configuration, and applying fixed boundary conditions at the beam base, the following force-displacement expressions may be derived for the beam-tip.

$$\theta_r^o = \frac{R_o^2}{2}\left[\frac{(1-\cos\beta_o)^2}{GI_t} + \frac{\sin^2\beta_o}{EI_b}\right]F_z^o + \frac{R_o}{2}\left[\frac{\beta_o - \cos\beta_o\sin\beta_o}{GI_t} + \frac{\beta_o + \cos\beta_o\sin\beta_o}{EI_b}\right]M_r^o + \frac{R_o}{2}\left[-\frac{\sin^2\beta_o}{GI_t} + \frac{\sin^2\beta_o}{EI_b}\right]M_\beta^o$$

$$\theta_\beta^o = \frac{R_o^2}{2}\left[\frac{\beta_o - 2\sin\beta_o + \cos\beta_o\sin\beta_o}{GI_t} + \frac{\beta_o - \cos\beta_o\sin\beta_o}{EI_b}\right]F_z^o + \frac{R_o}{2}\left[-\frac{\sin^2\beta_o}{GI_t} + \frac{\sin^2\beta_o}{EI_b}\right]M_r^o$$
$$+\frac{R_o}{2}\left[\frac{\beta_o + \cos\beta_o\sin\beta_o}{GI_t} + \frac{\beta_o - \cos\beta_o\sin\beta_o}{EI_b}\right]M_\beta^o$$

$$u_z^o = \frac{R_o^3}{2}\left[\frac{3\beta_o - 4\sin\beta_o + \cos\beta_o\sin\beta_o}{GI_t} + \frac{\beta_o - \cos\beta_o\sin\beta_o}{EI_b}\right]F_z^o + \frac{R_o^2}{2}\left[\frac{(1-\cos\beta_o)^2}{GI_t} + \frac{\sin^2\beta_o}{EI_b}\right]M_r^o$$
$$+\frac{R_o^2}{2}\left[\frac{\beta_o - 2\sin\beta_o + \cos\beta_o\sin\beta_o}{GI_t} + \frac{\beta_o - \cos\beta_o\sin\beta_o}{EI_b}\right]M_\beta^o$$

Assuming a pure Z-direction displacement of the diaphragm flexure, for example, in the case of the linear bearing where the X and Y direction rotations are negligibly small, the above general results may be used to compare the traditional and symmetric geometries of Fig.1a and 1c, respectively. For the first case, assuming four simple curved-beam flexure units and β_o=*90°*, the Z displacement is given by

$$u_z^o = \frac{R_o^3}{8GI_t}\left[\frac{\pi^2(EI_b + GI_t) + 2\pi(EI_b - GI_t) - 16EI_b}{\pi(EI_b + GI_t) + 2(EI_b - GI_t)}\right]F_z^o = \frac{R_o^3}{8GI_t}\left[\frac{3.59GI_t + 0.15EI_b}{1.14GI_t + 5.14EI_b}\right]F_z^o$$

The parasitic rotation of the diaphragm may be estimated by assuming constant beam arc-length

$$\frac{u_\beta^o}{R_o} = -\frac{2}{3}\left(\frac{u_z^o}{R_o}\right)^2\left[\frac{7.46G^2I_t^2 + 0.68GI_tEI_b + 0.016E^2I_b^2}{(3.59GI_t + 0.15EI_b)^2}\right]$$

As expected, this parasitic error along the DOC has a quadratic kinematic dependence on the primary DOF motion. The above derivation for a simple curved-beam may be easily extended to a folded curved-beam. For the symmetric diaphragm, with 4 folded-beam pairs and β_o=*45°*, the force-displacement relationship is given by

$$u_z^o = \frac{R_o^3}{4GI_t}\left[\frac{5.87G^2I_t^2 + 0.37GI_tEI_b + 0.003E^2I_b^2}{1.87G^2I_t^2 + 35.74GI_tEI_b + 1.87E^2I_b^2}\right]F_z^o$$

Because of the symmetric geometry, there is no kinematic parasitic rotation of the diaphragm in this case. Furthermore, for the same diameter, this design is approximately twice as compliant as the previous one. This closed-form analysis provides the basis for determining the force-displacement characteristics of various diaphragm flexures and facilitates the design of other flexure systems based on these modules.

Conclusions and Future Work

The analysis presented here captures only the purely elastic and kinematic terms in the force-displacement characteristics of the curved-beam. Non-linear elastokinematic terms that arise due to the application of force-equilibrium conditions in the deformed configuration are key in determining the constraint properties of the curved-beam flexure module. When incorporated in the analysis of the diaphragm flexure and the subsequent linear bearing or flexible coupling, these elastokinematic terms are pivotal in accurately predicting the tradeoffs between DOF and DOC, and therefore the true performance of the mechanisms. Ongoing research includes the closed-form quantification of these elastokinematic effects, thermal and dynamic analyses, and damping design. Test prototypes of the proposed flexure designs have been fabricated using water-jet machining and experiments to validate the analytical predictions are been planned.

References:

1. S. Awtar, A.H. Slocum, *Proc. ASME IDETC/CIE '05*, Paper 85440 (2005)
2. T.S. Donahoe, et al., US Patent No. 6,129,527 (1999)
3. H.Masuda, N.Okumua, US Patent No. 6,050,556 (2000)
4. R.B.Pan, et al., US Patent No. 5,492,313 (1996)
5. S. Awtar, *Analysis and Synthesis of Planer Kinematic XY Mechanisms,* Sc.D. Thesis, Massachusetts Institute of Technology, Cambridge MA (1994)
6. S. Awtar, A.H. Slocum, US Patent App. 20040037626 (2004)